Supporting materials:

# Multifunctional Lignin-based Composite Ultra-Adhesive for Wood Processing

*Boxiang Zhan, Long Zhang, Yongqi Deng, Lifeng Yan**

Key Laboratory of Precision and Intelligent Chemistry, and Department of Chemical Physics, University of Science and Technology of China. Jinzai road 96, 230026, Hefei, Anhui, P.R.China.

Corresponding author: Lifeng Yan, Fax/Tel: +86-551-63606853; E-mail: lfyan@ustc.edu.cn

**Table S1.** adhesive strengths of our work and those of currently reported lignin-based phenolic resin adhesives

| Number | Raw material | Modifification methods | Bonding strength | Ref. |
|---|---|---|---|---|
| 1 | DES-lignin-furfural | Deep eutectic solvent | 5.71MPa | Our work |
| 2 | Commercial phenol-formaldehyde | No | 4.60MPa | 11 |
| 3 | Lignin-formaldehyde | No | 4MPa | 11 |
| 4 | Lignin-glyoxal | No | 3.9MPa | 11 |
| 5 | Acetone soluble lignin-formaldehyde | Fractionation | 4.4MPa | 2 |
| 6 | Lignin-phenol-formaldehyde (50 %) | No | 3.46MPa | 3 |
| 7 | Lignin-phenol-formaldehyde (60 %) | Demethylation(DMF) | 2.28MPa | 13 |
| 8 | Lignin-phenol-formaldehyde (50 %) | Demethylation(HBr) | 0.85MPa | 14 |
| 9 | Lignin-phenol-formaldehyde (50 %) | Demethylation(HI) | 0.88MPa | 14 |
| 10 | Kraft lignin-formaldehyde (Hardwood) | No | 1.8MPa | 8 |
| 11 | Kraft lignin-formaldehyde (Softwood) | No | 2.6MPa | 8 |
| 12 | Organosolv lignin-formaldehyde (Hardwood) | No | 2.0MPa | 8 |
| 13 | Soda lignin-formaldehyde (Wheta straw) | No | 2.3MPa | 8 |
| 14 | Organosolv lignin-formaldehyde (Corn stover) | No | 2.4MPa | 8 |
| 15 | Enzymatic hydrolysis lignin-formaldehyde (Corn stover) | No | 3.2MPa | 8 |

**Table S2** IR characteristic peaks of furfural

| IR/$cm^{-1}$ | Assignment |
|---|---|
| 1392 | Heteropentacyclic inner ring respiration with $C_4$-H,$C_5$-H antisymmetric shear,$C_2$-H,$C_6$-H antisymmetric shear |
| 1567 | Heteropentacyclic inner ring respiration with $C_2$-$C_3$, $C_4$-$C_5$ antisymmetric shear,$C_3$-H, $C_4$-H antisymmetric shear |
| 2811/2855 | Telescopic vibration of $C_6$-H |
| 3136 | $C_3$-H, $C_4$-H antisymmetric stretching |

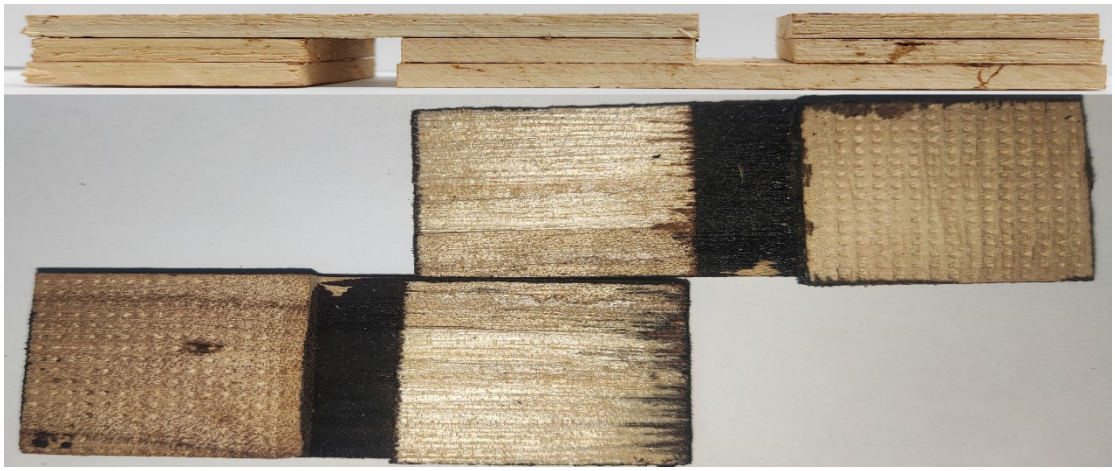

**Figure S1** Fracture of three-layer shear specimen Physical drawing

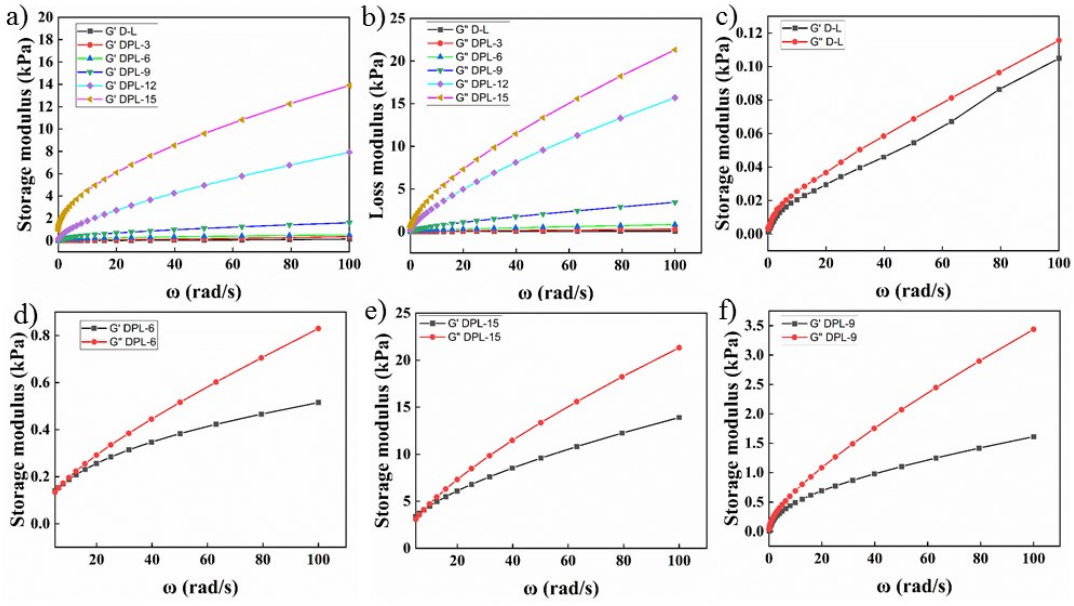


**Figure S2** Modulus plots of lignin depolymerized by DES (D-L) and adhesives prepared at different reaction times (DLF-3,6,9,12,15). a) Energy storage modulus; b) Loss modulus.

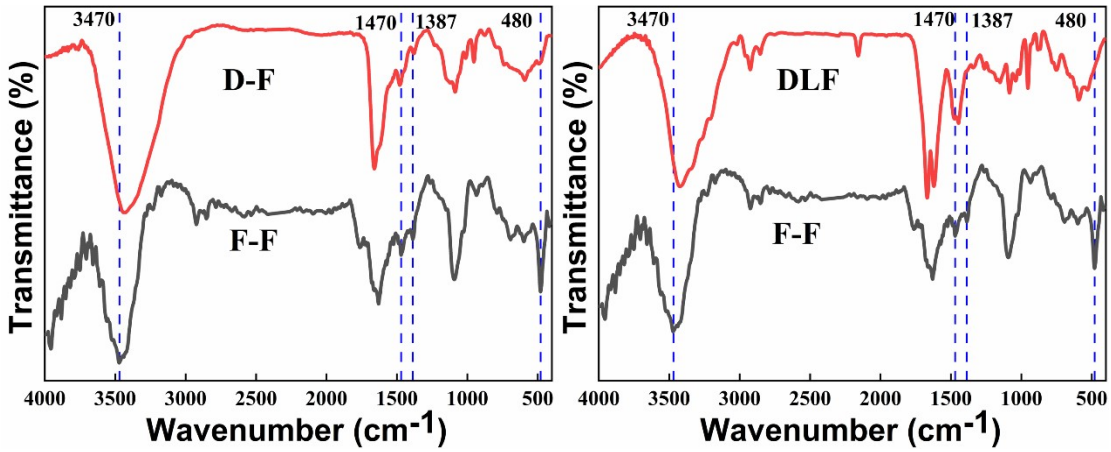


**Figure S3.** IR spectra of F-F, DLF, D-F

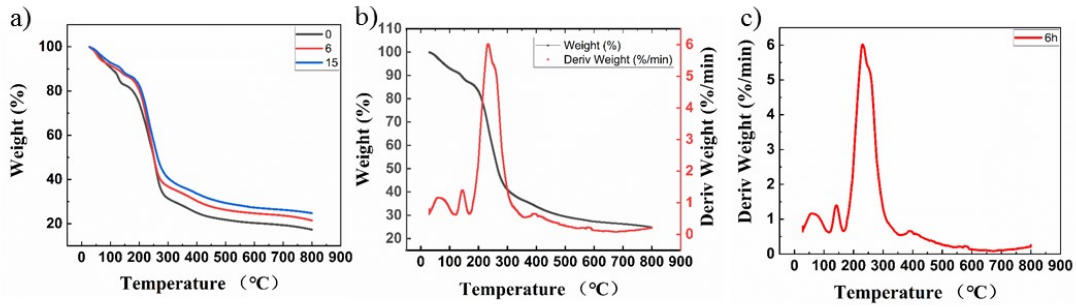


**Figure S4.** TGA curves of adhesives with reaction times of 0, 6, 15 h; TGA and DTG

curves of adhesives with reaction times of 6 h; DTG curves of adhesives with reaction times of 6 h.

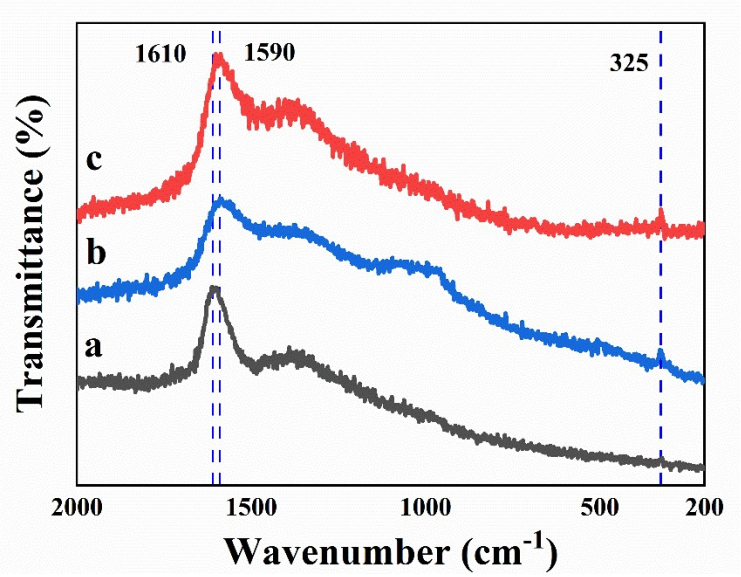


**Figure S5** Raman spectra of wood (a), DLF-6 (b) and wood penetrated by DLF-6 (c)

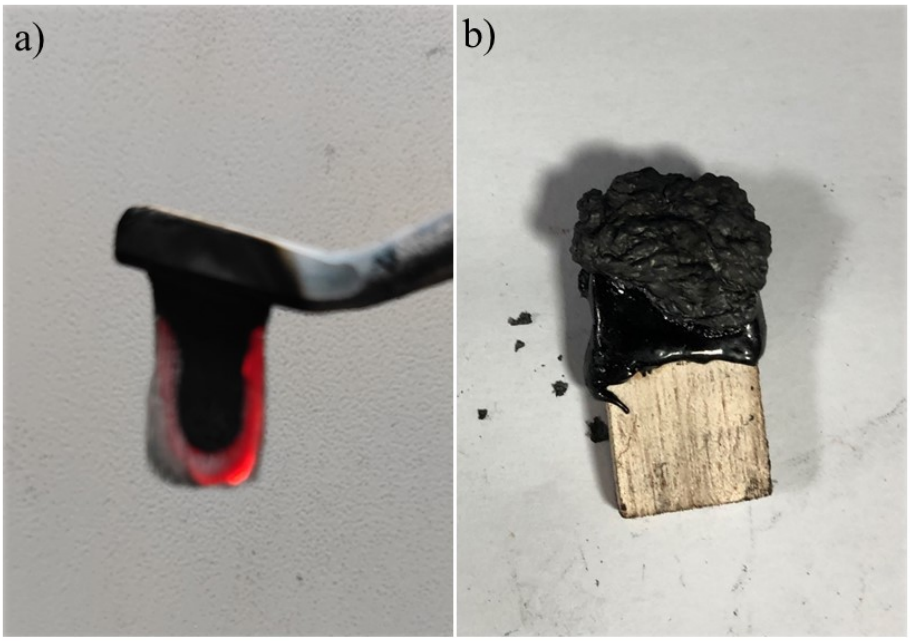


**Figure S6** a) Picture of untreated tung wood sheet after vertical burning test; b) Picture of tung wood sheet coated with DLF-6 adhesive after vertical burning test.

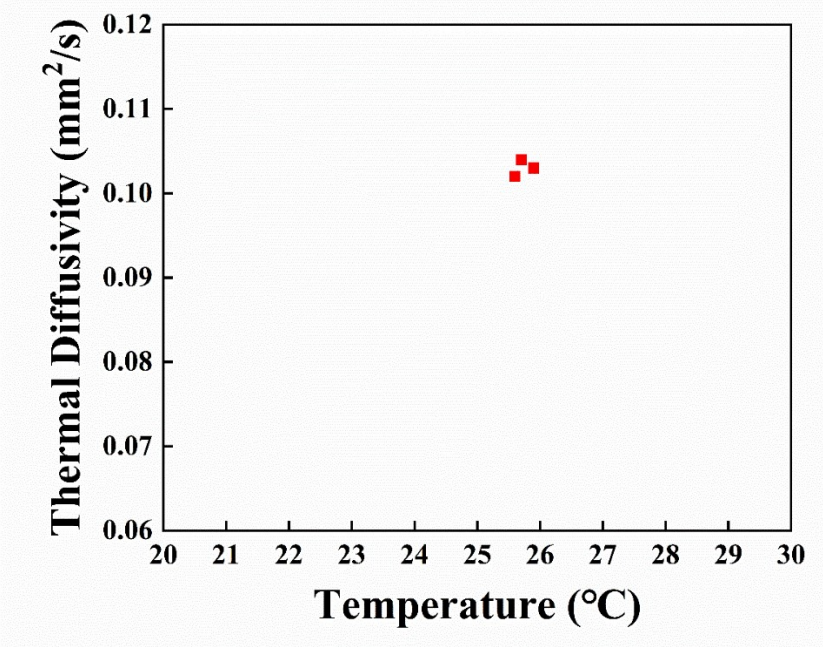


**Figure S7** Thermal diffusion coefficient of DLF-6.

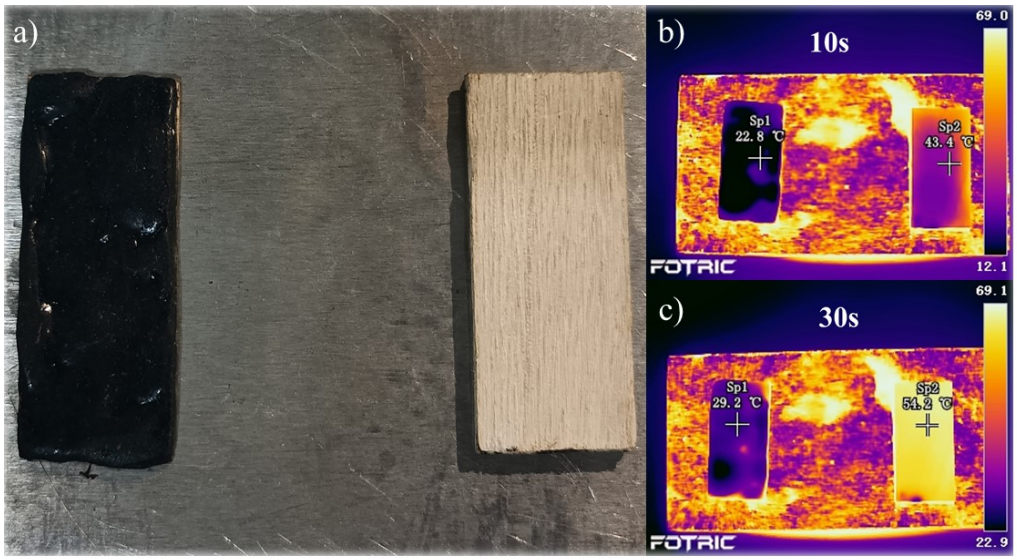


**Figure S8.** Recording of surface temperatures of DLF-6 samples and control samples located on a hot iron plate using infrared thermography. a) Sample placed on the iron plate; b) Surface temperature of samples heated for 10 s; c) Surface temperature of samples heated for 30 s

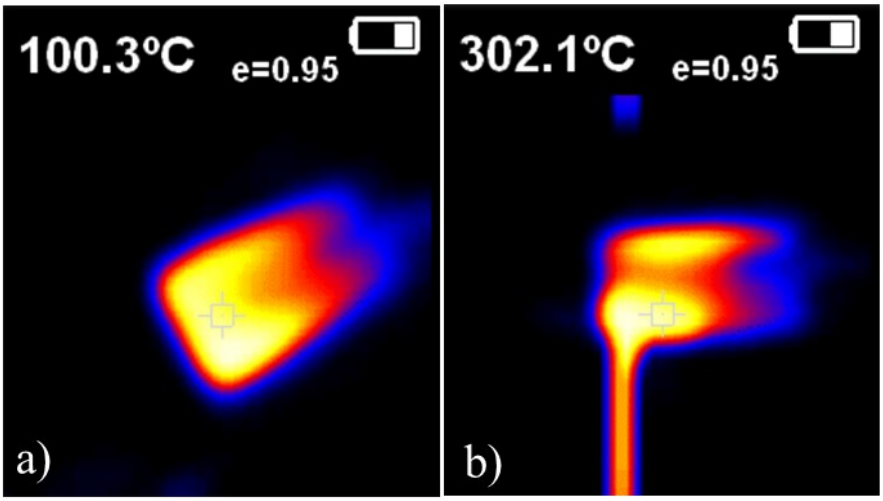


**Figure S9.** a) Temperature of the back side of the paulownia plate coated with DLF-6 adhesive when the front side was baked by an alcohol lamp for 10 s. b) Temperature of the back side of the paulownia plate without DLF-6 adhesive when the front side was baked by an alcohol lamp for 10 s.

A more detailed experiment was conducted to explore the thermal insulation performance of DLF-6 in a more visual way. We applied DLF-6 to a 1 mm thick paulownia plate with a coating thickness of 1 mm, and then stacked two 1 mm thick paulownia plates to the same thickness as the DLF-6 coated paulownia plate and used them as a control group. Two samples were placed on a hot iron plate and the frontal temperature was measured with an infrared thermographic camera after heating for 10 and 30 seconds, respectively (Figure S6a). It could be seen that at 10 s, the surface temperature of the paulownia plate coated with DLF-6 was 22.8°C, while the surface temperature of the control sample was 43.4°C (Figure S6b). At 30 s of heating, the surface of the DLF-6 sample was only 29.2°C, while the surface temperature of the control sample was 54.2°C (Figure S6c). Clearly, the DLF-6 adhesive has heat

insulation properties. Then, an alcohol lamp was used to heat the surface of the sample coated with DLF-6 for 10 s, and then the temperature of its backside was recorded with an infrared thermographer. At the same time, samples without DLF-6 adhesive applied were used as a control group and the same tests were performed. The temperature of the back side of the sample coated with DLF-6 was 100°C while the back side of the control sample was 300°C (Figure S7), indicating that the DLF-6 adhesive has superior thermal insulation properties at high temperatures.

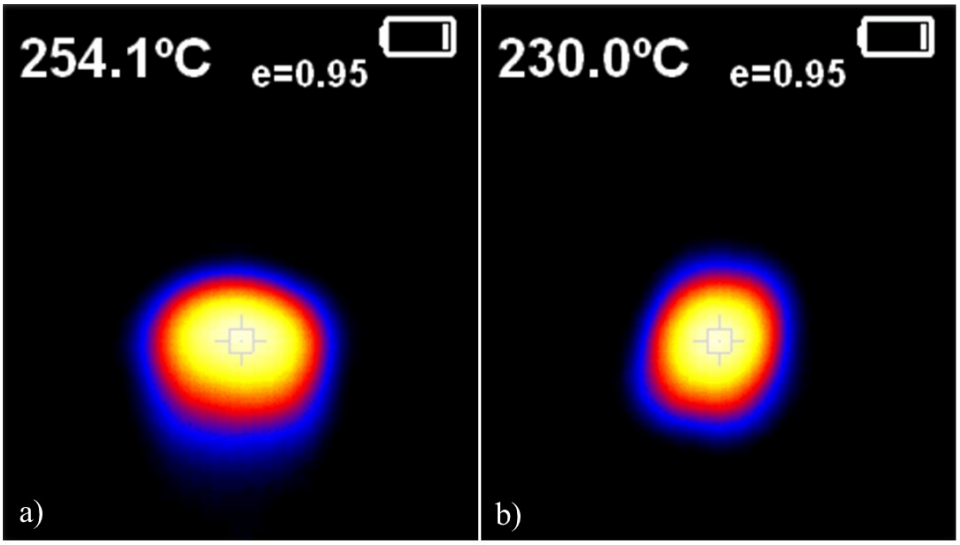


**Figure S10.** a) Temperature of DLF-6 adhesive after being irradiated by 808 nm laser for 131 s; b) Temperature of DLF-9 adhesive after being irradiated by 808 nm laser for 177 s.

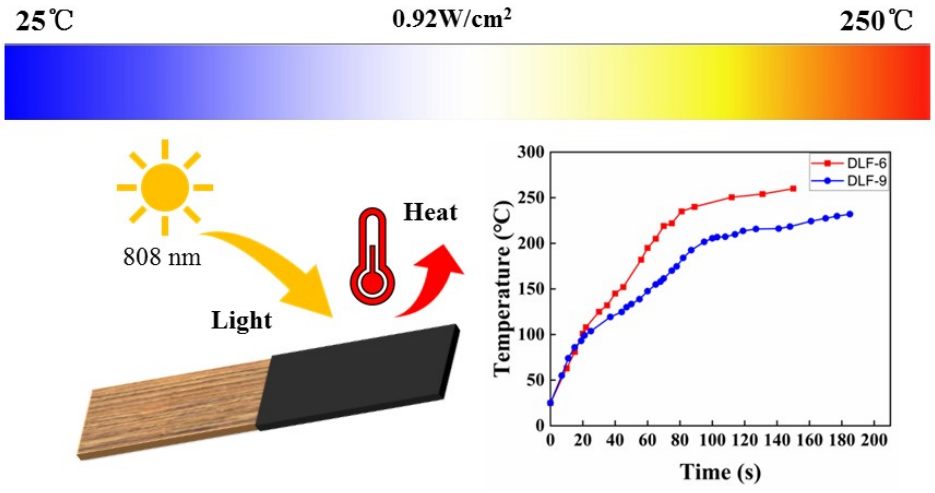


**Figure S11.** Temperature versus time curves of DLF-6 and DLF-9 under illumination.

**Photothermal properties.** Since lignin has more excellent photothermal properties, we guessed that DLF might inherit the photothermal properties of lignin. Therefore, we used an 808 nm laser with a light intensity of 0.92 W/cm$^2$ to irradiate the surface of DLF-6 adhesive and DLF-9 adhesive, and the temperature of DLF-6 and DLF-9 at different moments to plot the temperature variation with irradiation time was recorded by an infrared thermal imager (Figure S9). The graph shows that DLF-6 outperforms DLF-9 in terms of temperature rise rate and maximum temperature (Figure S8). Therefore, it can be concluded that the degree of cross-linking of DLF adhesive increases, and its photothermal performance decreases with the increase in reaction time. Due to the excellent photothermal properties of this adhesive, light can be used to replace the heat during the hot-pressing process. Under a certain light intensity, DLF-6 adhesive can meet the temperature required for hot pressing, so it has the prospect of application where light can replace heating. It also has potential for application as a photothermal material.

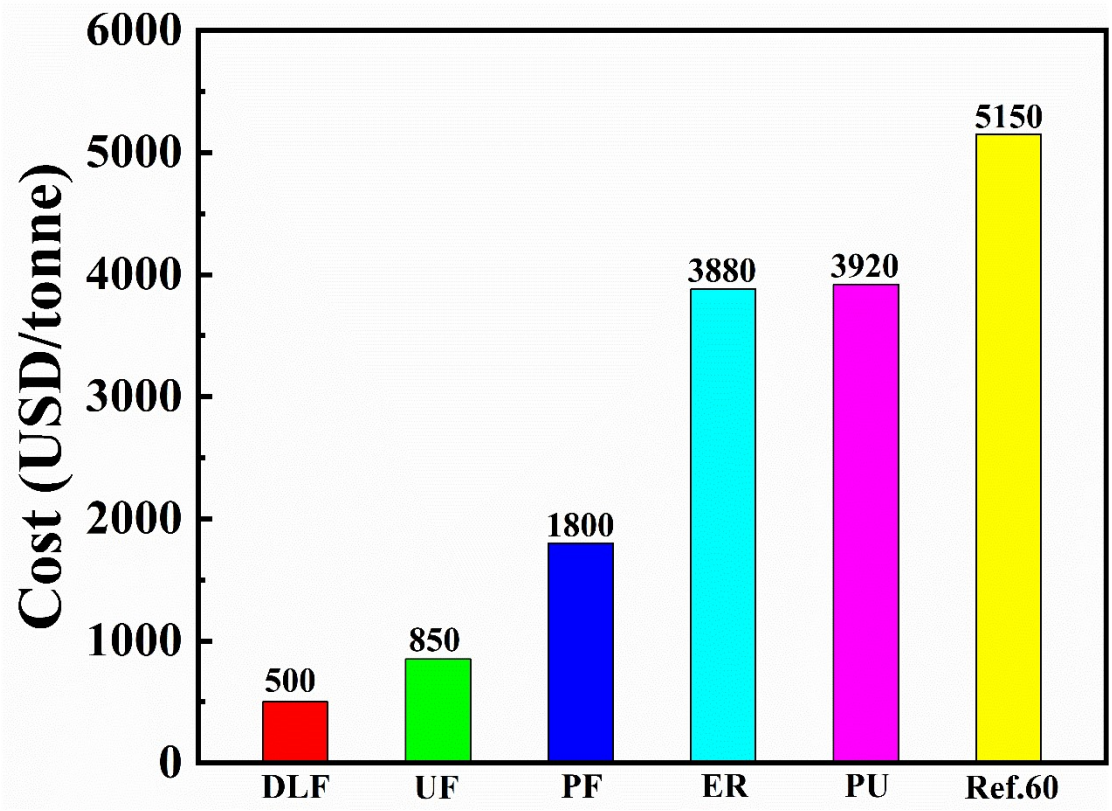


**Figure S12.** Cost comparison of different adhesives

Choline chloride (99.0%) at $684/metric ton (Hubei Rishengchang New Material Technology Co., Ltd.); Urea (99.0%) at $500/metric ton (Jiangsu Kolod Food Ingredients Co.,Ltd); Lignin (90.0%) at $100/metric ton (Healtang Biotech CO,Ltd); Furfural (99.0%) at $820/metric ton (Shanghai Lanrun Chemical Co., Ltd.); Potassium carbonate (99.0%) at $136/metric ton (Hubei Ju Sheng Technology Co., Ltd.); Phenolic resin (100%) market price at $1800/metric ton (Shanghai Tuhuang International Co.,Ltd). The above data are all from Guidechem Chemical Network.

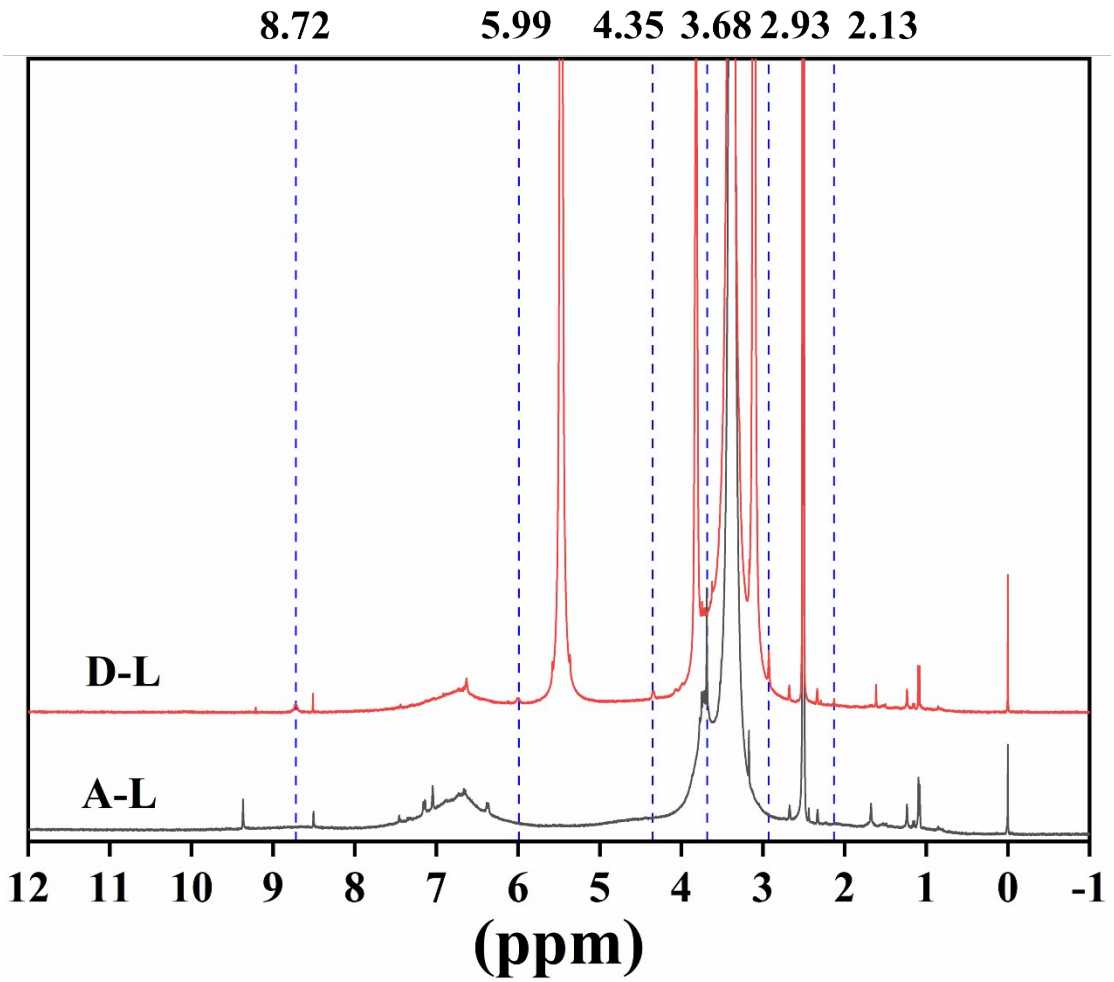


**Figure S13.** 1H NMR Characterization

The structural changes of A-L and D-L are evident from the 1H-NMR hydrogen spectra. Firstly, the sharp peaks at 5.47 ppm, 3.8 ppm, and 3.1 ppm in D-L are the signals of residual DES in lignin. Moreover, the sharp peak at 3.4 ppm is the proton model of water and the one at 2.5 ppm is the solvent signal. Secondly, the methoxy signal at 3.68 ppm, which disappeared in D-L, indicated that the DES had a demethoxylation effect on lignin, which was the same as the results in the literature. In general, aromatic phenolic hydroxyl groups tend to be lower field. 0.5-5.5 ppm for alcohol hydroxyls and 4-8 ppm for phenolic hydroxyls. In addition, phenolic hydroxyls

can also be seen in chemical shifts greater than 8. From the results, it can be seen that there are new signals in D-L at 2.13 ppm, 2.93 ppm, 4.35 ppm, 5.99 ppm and 8.72 ppm. These are signals generated by phenolic hydroxyls as well as alcohol hydroxyls, which suggests that DES deconvolutes lignin and there are a variety of phenolic hydroxyls as well as alcohol hydroxyls generated, which is in agreement with the results of the FTIR spectroscopy. It is worth mentioning that 8.0-6.2 ppm are attributed to the proton signals on the aromatic nuclei of guaiacyl unit and syringyl unit.

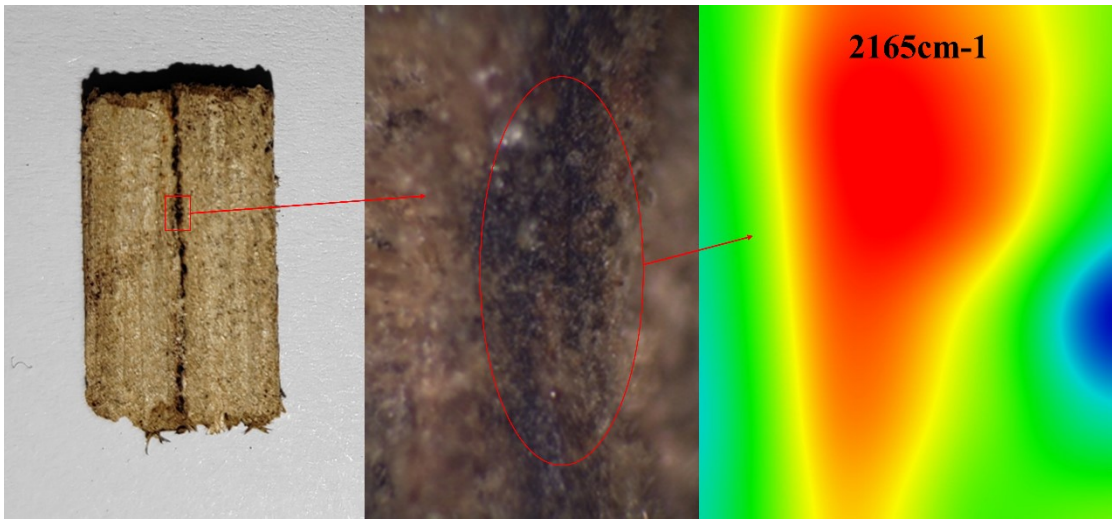


**Figure S14.** FTIR spectroscopic microscopic images